



Scholars Research Library

Der Pharmacia Lettre, 2016, 8 (4):255-264
(<http://scholarsresearchlibrary.com/archive.html>)



Evaluation of 2-thioxo-1,2-dihydroquinoline-4-carboxylic acid as corrosion inhibitor for carbon steel in 1M HCl

A.Elyoussfi¹, Y. Bouzian², A. Dafali¹, H. Elmsellem¹, R. Bouhfid³, R. Mehdaoui⁴,
K. Cherrak¹, E. M. Essassi², A. Zarrouk¹ and B. Hammouti¹

¹LCAE-URAC 18, Faculty of Science, First Mohammed University, PO Box 717, 60 000 Oujda, Morocco

²Laboratoire de Chimie Organique Hétérocyclique, URAC 21, Pôle de Compétences Pharmacochimie, Université Mohammed V, Faculté des Sciences, Av. Ibn Battouta, BP 1014 Rabat, Morocco

³Moroccan Foundation for Advanced Science, Innovation and Research (MASCIR), Institut of Nanomaterials and Nanotechnology, Rabat, Morocco

⁴Laboratoire de Génie chimique, Département de Génie des Procédés, Faculté de Technologie, Université de Blida 1, BP 270, Route de Soumaâ, 09000, Blida, Algérie

ABSTRACT

The inhibition effect of the 2-thioxo-1,2-dihydroquinoline-4-carboxylic (Q2) on carbon steel (CS) corrosion in 1 M HCl have been determined by electrochemical techniques like potentiodynamic polarization (PDP), electrochemical impedance spectroscopy studies (EIS) and weight loss measurements. The experimental results reveal that Q2 is an effective inhibitor with a maximum achievable inhibition efficiency of 95% at 10^{-3} M. The polarization curves indicated that Q2 behaved as a mixed-type inhibitor while the Nyquist plots revealed that the corrosion was a charge transfer controlled process. Moreover, the adsorption of Q2 was found to obey the Langmuir adsorption isotherm. Density functional theory (DFT) was employed for theoretical calculations.

Keywords: Quinoline derivative, Electrochemical investigation, Weight loss measurement, Corrosion inhibitor, Carbon steel, Quantum chemical.

INTRODUCTION

The corrosion of steel is a fundamental academic and industrial concern that has received a considerable amount of attention. Acid solutions are extensively used in many industrial processes such as acid pickling, industrial acid cleaning, oil-well acidizing, which leads to corrosive attack. In the past few years, numerous inhibitors have been investigated to study their inhibitive effect, as well as the relationship between inhibitor molecular structure and corresponding inhibition efficiency [1-4]. The majority of the well-known inhibitors are organic compounds containing heteroatoms, such as oxygen, nitrogen or sulphur, and multiple bonds, which allow an adsorption on the metal surface [5-34].

The inhibiting action of organic compounds on the corrosion of metals in acid media is usually related to their adsorption on the metal surface [35-37]. Adsorption results in an effective blocking of the active sites of metal dissolution and/or hydrogen evolution, thus diminishing the overall corrosion rate. The relationship between the adsorption of organic inhibitors and their molecular structure has attracted the attention of many investigators [38,39]. The presence of functional groups and the electron density distribution in the molecules of the organic substances are factors that strongly influence their adsorption behavior.

Therefore in the present work 2-thioxo-1,2-dihydroquinoline-4-carboxylic (Q2) is investigated as the inhibitor for carbon steel corrosion in 1 M HCl at 308 K. The inhibition effect of Q2 was evaluated by means of weight loss

measurement, potentiodynamic polarization, and electrochemical impedance spectroscopy. Quantum chemical calculations were further employed to explain the inhibition efficiency of Q2.

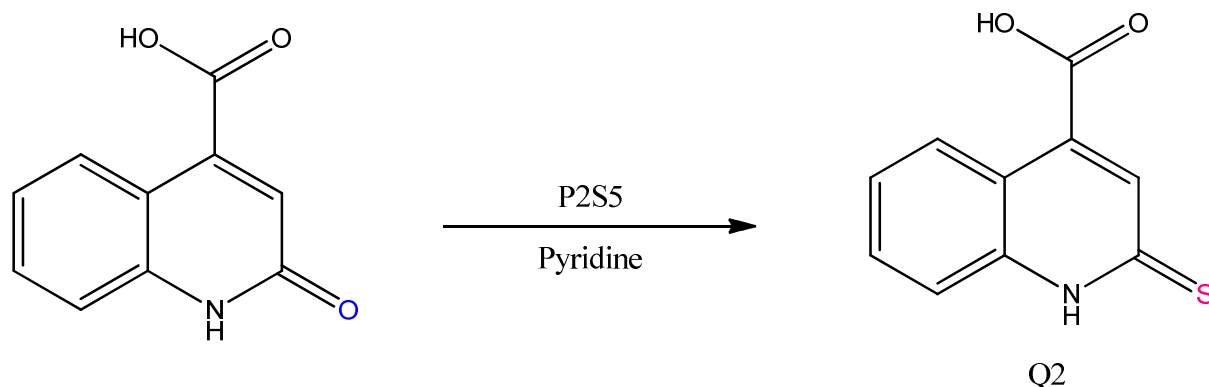
MATERIALS AND METHODS

Materials

The steel used in this study is a carbon steel (CS) (Euronorm: C35E carbon steel and US specification: SAE 1035) with a chemical composition (in wt%) of 0.370 % C, 0.230 % Si, 0.680 % Mn, 0.016 % S, 0.077 % Cr, 0.011 % Ti, 0.059 % Ni, 0.009 % Co, 0.160 % Cu and the remainder iron (Fe).

Synthesis

To a well-stirred solution of (5 g, 33.1mmol) 2-oxo-1,2-dihydroquinoline-4-carboxylic acid in 50 mL of dry pyridine was added (14.7 g, 33.1mmol) phosphorus pentasulfide. The reaction mixture is heated to reflux for 4 hours, the solid obtained is washed several times with hot water, dried and then purified in absolute ethanol. Recrystallization is carried out in the petroleum ether. The product obtained was characterized by ¹H NMR, ¹³C NMR.



Rdt = 90 %. ¹H NMR (DMSO-d₆): 7.41(s, 1H, CH); 7.28-8.5(m, 4H, CH_{Ar}). ¹³C NMR (DMSO-d₆): 121.6 (=CH); 117.2, 126.1, 127.0, 128.3 (CH_{Ar}); 122.7, 134.5, 140.2 (Cq); 191.4 (C=O); 166.1 (CO₂H). ESI-MS MH m/z = 206.23.

Solutions

The aggressive solutions of 1 M HCl were prepared by dilution of analytical grade 37% HCl with distilled water. The concentration range of 2-thioxo-1,2-dihydroquinoline-4-carboxylic (Q2) used was 10⁻⁶ M to 10⁻³ M.

Gravimetric study

Gravimetric experiments were performed according to the standard methods [40], the carbon steel sheets of 1 × 1 × 0.1 cm were abraded with a series of emery papers SiC (120, 600 and 1200) and then washed with distilled water and acetone. After weighing accurately, the specimens were immersed in a 100 mL beaker containing 250 mL of 1 M HCl solution with and without addition of different concentrations inhibitor. All the aggressive acid solutions were open to air. After 6 h of acid immersion, the specimens were taken out, washed, dried, and weighed accurately. In order to get good reproducibility, all measurements were performed few times and average values were reported to obtain good reproducibility. The inhibition efficiency (η_{WL}%) and surface coverage (θ) were calculated as follows:

$$C_R = \frac{W_b - W_a}{At} \quad (1)$$

$$\eta_{WL} (\%) = \left(1 - \frac{w_i}{w_0} \right) \times 100 \quad (2)$$

$$\theta = \left(1 - \frac{w_i}{w_0} \right) \quad (3)$$

where W_b and W_a are the specimen weight before and after immersion in the tested solution, w_0 and w_1 are the values of corrosion weight losses of carbon steel in uninhibited and inhibited solutions, respectively, A the total area of the carbon steel specimen (cm^2) and t is the exposure time (h).

Electrochemical measurements

Electrochemical impedance spectroscopy

The electrochemical measurements were carried out using Volta lab (Tacussel- Radiometer PGZ 100) potentiostat and controlled by Tacussel corrosion analysis software model (Voltmaster 4) at under static condition. The corrosion cell used had three electrodes. The reference electrode was a saturated calomel electrode (SCE). A platinum electrode was used as auxiliary electrode of surface area of 1 cm^2 . The working electrode was carbon steel. All potentials given in this study were referred to this reference electrode. The working electrode was immersed in test solution for 30 minutes to establish steady state open circuit potential (E_{ocp}). After measuring the E_{ocp} , the electrochemical measurements were performed. All electrochemical tests have been performed in aerated solutions at 308 K. The EIS experiments were conducted in the frequency range with high limit of 100 kHz and different low limit

0.1 Hz at open circuit potential, with 10 points per decade, at the rest potential, after 30 min of acid immersion, by applying 10 mV ac voltage peak-to-peak. Nyquist plots were made from these experiments. The best semicircle can be fit through the data points in the Nyquist plot using a non-linear least square fit so as to give the intersections with the x -axis.

The inhibition efficiency of the inhibitor was calculated from the charge transfer resistance values using the following equation:

$$\eta_z \% = \frac{R_{ct}^i - R_{ct}^\circ}{R_{ct}^i} \times 100 \quad (4)$$

where, R_{ct}° and R_{ct}^i are the charge transfer resistance in absence and in presence of inhibitor, respectively.

Potentiodynamic polarization

The electrochemical behaviour of carbon steel sample in inhibited and uninhibited solution was studied by recording anodic and cathodic potentiodynamic polarization curves. Measurements were performed in the 1 M HCl solution containing different concentrations of the tested inhibitor by changing the electrode potential automatically from -600 to -300 mV versus corrosion potential at a scan rate of 1 mV s^{-1} . The linear Tafel segments of anodic and cathodic curves were extrapolated to corrosion potential to obtain corrosion current densities (I_{corr}). From the polarization curves obtained, the corrosion current (I_{corr}) was calculated by extrapolation of the linear segments of cathodic and anodic Tafel curves.

The inhibition efficiency was evaluated from the measured I_{corr} values using the relationship:

$$\eta_{Tafel} \% = \frac{I_{corr}^\circ - I_{corr}^i}{I_{corr}^\circ} \times 100 \quad (5)$$

where, I_{corr}° and I_{corr}^i are the corrosion current density in absence and presence of inhibitor, respectively.

Quantum chemical calculations

Complete geometry optimization of the inhibitor molecules were performed using density functional theory (DFT) with Beck's three-parameter exchange functional along with LeeYangeParr non-local correlation functional (B3LYP) with 6-1G* basis set using the Gaussian 03 programme package [41]. Frontier molecular orbitals (HOMO and LUMO) were used to interpret the adsorption of inhibitor molecules on the metal surface. According to DFT-Koopman's theorem [42,43], the ionization potential (I) is approximated as the negative of the highest occupied molecular orbital energy (E_{HOMO}) and the negative of the lowest unoccupied molecular orbital energy (E_{LUMO}) is related to the electron affinity (A).

$$I = -E_{HOMO} \quad (6)$$

$$A = -E_{LUMO} \quad (7)$$

Natural bond orbital (NBO) analysis [44] was performed to evaluate the electron density distributions. The electron density plays an important role in calculating the chemical reactivity parameters. The global reactivities include electronegativity (χ), global hardness (η) and the global softness (σ). They can be calculated from the following equations:

$$\chi = \frac{I + A}{2} \quad (8)$$

$$\eta = \frac{I - A}{2} \quad (9)$$

$$\sigma = \frac{1}{\eta} = -\frac{2}{E_{HOMO} - E_{LUMO}} \quad (10)$$

The number of transferred electrons (ΔN) was also calculated depending on the quantum chemical method [45,46] by using the equation;

$$\Delta N = \frac{\chi_{Fe} - \chi_{inh}}{2(\eta_{Fe} + \eta_{inh})} \quad (11)$$

Where χ_{Fe} and χ_{inh} denote the absolute electronegativity of iron and inhibitor molecule η_{Fe} and η_{inh} denote the absolute hardness of iron and the inhibitor molecule respectively. In this study, we use the theoretical value of $\chi_{Fe} = 7.0 \text{ eV mol}^{-1}$ and $\eta_{Fe} = 0 \text{ eV mol}^{-1}$, for calculating the number of electron transferred.

RESULTS AND DISCUSSION

Weight loss studies

The 2-thioxo-1,2-dihydroquinoline-4-carboxylic (Q2) showed maximum inhibition efficiency of 95.4 % in HCl at an optimum concentration of 10^{-3} M. Further increase in inhibitor concentration did not cause any significant change in the performance of the inhibitor. The values of percentage inhibition efficiency ($\eta_{WL}\%$) and corrosion rate (C_R) obtained from weight loss method at different concentrations of Q2 at 308 K are summarized in Table 1.

Table 1: Parameters obtained from gravimetric measurements for carbon steel in 1 M HCl containing different concentrations of Q2 at 308 K

Medium	Conc (M)	C_R (mg cm ⁻² h ⁻¹)	η_{WL} (%)	θ
Blank	1.0	0.910	—	—
	10^{-3}	0.041	95.4	0.954
Q2	10^{-4}	0.064	93.0	0.930
	10^{-5}	0.088	88.8	0.888
	10^{-6}	0.162	82.2	0.822

From table 1 it is clear that increase of inhibitor concentrations caused a decrease in the weight loss as well as corrosion rate of carbon steel.

Adsorption isotherm and standard adsorption free energy

It is well established that the first step in corrosion inhibition of metals and alloys is the adsorption of organic inhibitor molecules at the metal/solution interface and that the adsorption depends on the molecule's chemical composition, the temperature and the electrochemical potential at the metal/solution interface. In fact, the solvent water molecules could also adsorb at metal/solution interface. So the adsorption of organic inhibitor molecules from the aqueous solution can be regarded as a quasi-substitution process between the organic compounds in the aqueous phase [$Org_{(sol)}$] and water molecules at the electrode surface [$H_2O_{(ads)}$] [47]



where x, the size ratio, is the number of water molecules displaced by one molecule of organic inhibitor. x is assumed to be independent of coverage or charge on the electrode [48].

Basic information on the interaction between the inhibitor and the alloy surface can be provided by the adsorption isotherm. In order to obtain the isotherm, the fractional coverage values θ as a function of inhibitor concentration (C_{inh}) must be obtained. It is well known that θ can be obtained from the $\eta_{WL}\%/100$ ratio. Attempts were made to fit the θ values to various isotherms including Langmuir, Temkin, Frumkin and Flory-Huggins. Many adsorption isotherms were plotted and the Langmuir adsorption isotherm was found to be the best description of the adsorption behavior of the studied inhibitors. According to this isotherm, θ is related to equilibrium adsorption constant (K_{ads}) and C_{inh} by the relation

$$\frac{C_{inh}}{\theta} = \frac{1}{K_{ads}} + C_{inh} \quad (13)$$

Figure 1 shows the plot of C_{inh}/θ vs. C_{inh} and the expected linear relationship is obtained. The value of the regression coefficient (R^2) confirmed the validity of this approach. The slope of this straight line is 1.05, suggesting that adsorbed inhibitor molecules form monolayer on the carbon steel surface and that is no interaction among the adsorbed inhibitor molecules. On the other hand, the equilibrium constant of adsorption is related to the standard energy of adsorption (ΔG_{ads}°) by the relation [49]

$$K_{ads} = \left(\frac{1}{55.5} \right) \exp \left(-\frac{\Delta G_{ads}^\circ}{RT} \right) \quad (14)$$

where R is the gas constant, T is the absolute temperature of experiment and the constant value of 55.5 is the concentration of water in solution in mol L⁻¹ [50].

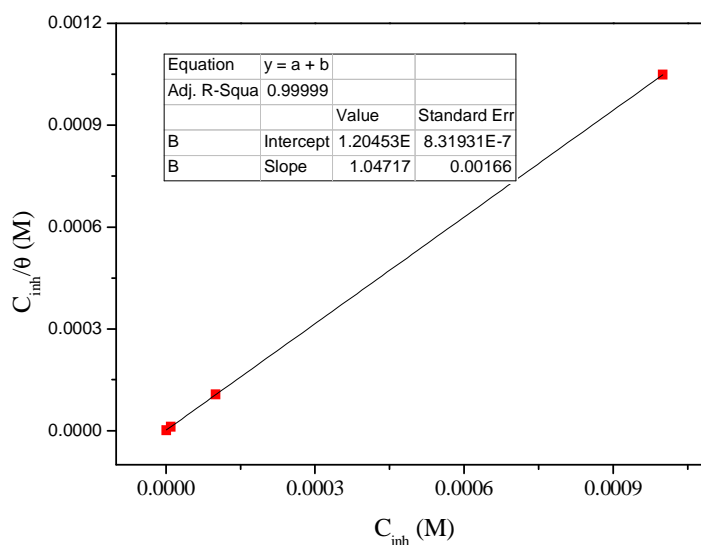


Figure 1: Langmuir adsorption of Q2 on the carbon steel surface in 1 HCl solution

The values of thermodynamic parameters are listed in Table 1. The values of K_{ads} and ΔG_{ads}° increase with increasing the inhibitor concentration, suggesting stronger interaction between inhibitor molecules and the iron surface atoms. The high value of these parameters indicates that stronger and more stable adsorbed layer is formed at carbon steel/acid solution interface, which results in the higher inhibition efficiency [51]. Generally, ΔG_{ads}° values of -20 kJ mol^{-1} or higher are associated with an electrostatic interaction between charged molecules and charged metal surface (physisorption); those of -40 kJ mol^{-1} or lower involve charge sharing or transfer from the inhibitor molecules to the metal surface to form a coordinate covalent bond (chemisorptions) [52]. ΔG_{ads}° is equal to $-45.18 \text{ kJ mol}^{-1}$, this high value of ΔG_{ads}° shows that in the presence of 1 M HCl chemisorption of Q2 may occur.

Table 1: Thermodynamic parameters for the adsorption of Q2 in 1.0 M HCl on the carbon steel at 308 K

Inhibitor	Slope	$K_{ads} (M^{-1})$	R^2	$\Delta G_{ads}^{\circ} (kJ/mol)$
Q2	1.05	830199.33	0.99999	-45.18

Potentiodynamic polarization

Polarization curves for carbon steel at various concentrations of cimetidine in are shown in Figure 2. It is clear from the potentiodynamic curves that the presence of cimetidine, in acid solution, decreases the corrosion rate. The decrease in I_{corr} value is due to the adsorption of the inhibitor molecules. It is observed that both the cathodic and anodic reactions are suppressed with the addition of Q2 which suggests it inhibit both anodic dissolution and cathodic hydrogen evolution reaction. Electrochemical corrosion parameters i.e. corrosion potential (E_{corr}), cathodic and corrosion current density (I_{corr}) obtained from the Tafel extrapolation of the polarization curves along with inhibition efficiency are given in Table 2.

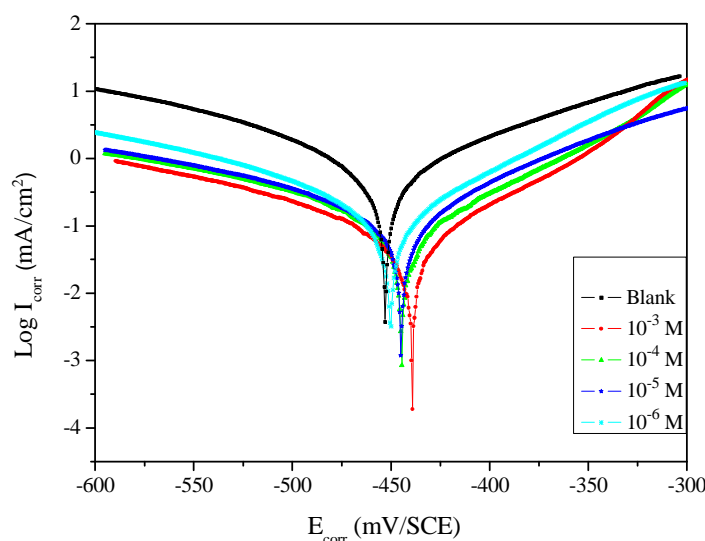


Figure 2: Potentiodynamic polarization curves for carbon steel in 1 M HCl in absence and presence of various concentrations of Q2 at 308 K

Table 2: Potentiodynamic polarization parameters for carbon steel in absence and presence of Q2 in 1 M HCl

Medium	Conc (M)	$-E_{corr} (mV_{SCE})$	$-\beta_c (mV/dec)$	$I_{corr} (\mu A cm^{-2})$	$\eta_{Tafel} (%)$
Blank	1.0	453	143.0	1559.0	—
Q1	10^{-3}	444	123.0	69.8	95
	10^{-4}	439	152.6	159	90
	10^{-5}	444	156.1	223	86
	10^{-6}	450	147.6	347	78

From table 2, the reduction in I_{corr} is pronounced more and more with the increasing inhibitor concentration. The increased inhibition efficiency with the inhibitor concentration indicates that the tested organic compound acts by adsorbing on the carbon steel surface. The presence of Q2 in 1 M HCl solution shifts the corrosion potential slightly towards more positive potentials with respect to the corrosion potential observed in the uninhibited solution. The largest displacement of E_{corr} was about 14 mV (< 85 mV), which indicates that Q2 might act as a mixed-type inhibitor with predominant anodic effectiveness [53]. The cathodic branch of polarization curves was given rise to parallel lines. This shows that the addition of Q2 to the 1 M HCl solution does not change the cathodic hydrogen evolution mechanism and the decrease of H^+ ions on the surface of carbon steel take place mainly through a charge transfer mechanism [54]. The inhibition effect of Q2 may be caused by the simple blocking effect, namely the reduction of reaction area on the corroding surface.

Electrochemical impedance spectroscopy (EIS) measurements

Electrochemical impedance spectroscopy (EIS) is an effective method for corrosion studies of metallic materials. The effect of Q2 concentration on the impedance spectra of carbon steel in 1 M HCl solutions at 308 K is recorded in Fig. 3(Nyquist plots). It is clear to see that the impedance spectra are significantly changed with addition of different Q2 concentration. From the Nyquist plots, it was also observed that, even the presence of Q2 does not alter

the style of impedance plots, thus indicating the addition of Q2 does not change the mechanism for the dissolution of carbon steel in 1 M HCl solution [55-57].

The impedance diagrams show only one capacitive loop represented by slightly depressed semicircle which indicates that the corrosion of carbon steel in 1 M HCl solution is mainly controlled by charge transfer process and formation of a protective layer on the carbon steel surface. The diameter of the capacitive loop increases with the increase of Q2 concentration proposing that the formed inhibitive film was strengthened by the addition of Q2 [58]. The depressed semicircles are generally attributed to the frequency dispersion as well as roughness and inhomogeneities of solid surface, and mass transport process [59], distribution of the active sites, adsorption of inhibitors [60-64].

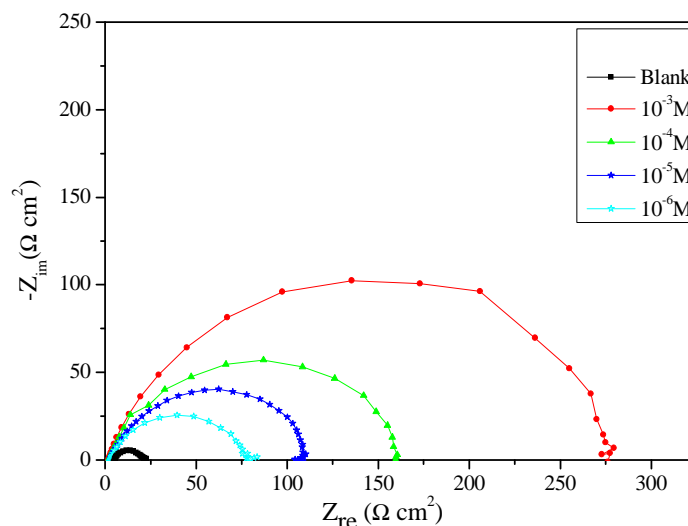


Figure 3: Nyquist plots for the carbon steel in absence and presence of different concentrations of Q2 at 308 K

The main parameters deduced from the analysis of Nyquist diagram are: The resistance of charge transfer R_{ct} (diameter of high frequency loop). The capacity of double layer C_{dl} which is defined as:

$$C_{dl} = \frac{1}{2\pi f_{max} R_{ct}} \quad (15)$$

Where f is the frequency.

The impedance data such as C_{dl} , R_{ct} , f_{max} and $\eta_z\%$ are given in Table 3. From the impedance data given in Table 3, we conclude that:

It is clear from Table 3 that the C_{dl} values decrease and R_{ct} increase after addition of inhibitor concentrations. The decrease in the C_{dl} is due to the decrease in local dielectric constant and/or an increase in the thickness of electrical double layer is attributed to the gradual replacement of water molecules and other ions originally adsorbed on the surface by the adsorption of inhibitor molecules on the carbon steel surface, thereby causing the increase in R_{ct} values [65]. Inhibition efficiency of the studied inhibitor increases due to the formation of a protective film of Q2 on the carbon steel surface. This film creates a barrier between carbonsteel and aggressive solution [66].

Table 3: Electrochemical impedance parameters for carbon steel in 1 M HCl in the absence and presence of Q2.

Medium	Conc (M)	R_{ct} ($\Omega \text{ cm}^2$)	C_{dl} ($\mu\text{F cm}^{-2}$)	f_{max} (Hz)	η_z (%)
Blank	1.0	16.6	200	48.0	—
Q2	10^{-3}	275	57.8	10.0	94
	10^{-4}	159	63.1	15.9	89
	10^{-5}	107	73.8	20.0	84
	10^{-6}	76	83.7	40.0	78

Quantum chemical study

It is well known that molecular structure of the inhibitor plays a vital role in determining its mode of adsorption on the corroded surface. To investigate the correlation between molecular structure of 2-thioxo-1,2-dihydroquinoline-4-carboxylic (Q2) and its inhibition effect, quantum chemical parameters has been performed.

Protection efficiency of inhibitors depends on the electronic properties of the corrosion inhibitors such as: highest occupied molecular orbital (HOMO), the lowest unoccupied molecular orbital (LUMO). It has been reported [67-69] that the higher the HOMO energy of the inhibitor the greater the trend of offering electrons to unoccupied d orbital of the metal, and the higher the corrosion efficiency. In addition, the lower the LUMO energy the easier the acceptance of electrons from metal surface [70]. The frontier molecular orbital density distributions of HOMO and LUMO for Q2 were shown in Figure 4. The calculated quantum chemical parameters for Q2 were listed in Table 4.

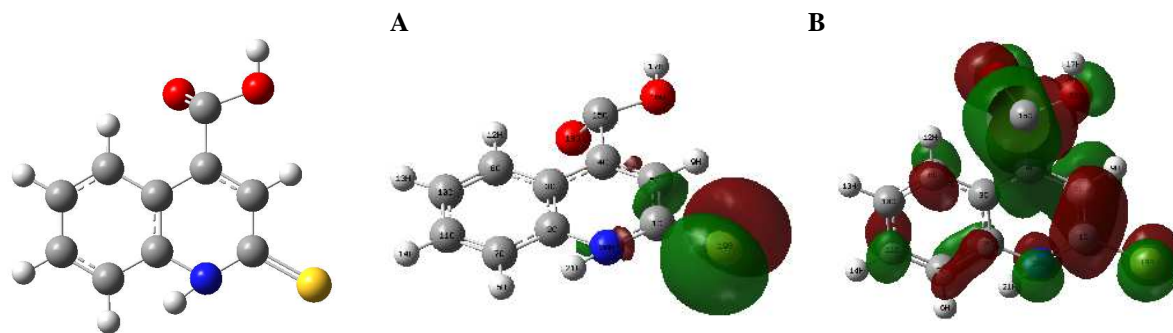


Figure 4: The frontier molecular orbital density distribution for Q2: (A) HOMO, (B) LUMO

Table 4: The calculated quantum chemical parameters for Q2.

E_{HOMO} (eV)	E_{LUMO} (eV)	ΔE_{gap} (eV)	μ (debye)	I (eV)	A (eV)	ΔN
-8.2711	-2.1878	-6.0833	7.1421	8.2711	2.1878	0.2911

The ability of the molecules to donate the electrons to appropriate molecular orbitals is indicated by E_{HOMO} , whereas the E_{LUMO} indicates its ability to accept electrons. This could be simply donating electron density to form a bond (act as a Lewis base) or it could be oxidation. As the value of E_{HOMO} is higher, the easier is its ability to offer electrons to the unoccupied d-orbital of metal surface, and it results in maximum efficiency [71]. The difference between E_{HOMO} and E_{LUMO} results ΔE , i.e., $E_{HOMO} - E_{LUMO} = \Delta E$. The value of ΔE indicates the extent of inhibition efficiency. The smaller value of ΔE facilitates adsorption of the molecule and thus will cause higher inhibition efficiency, because the energy to remove an electron from the last occupied orbital will be low [72,73]. Mahendra Yadav et al. [74] reported the ΔE value in the range of 7.9 - 8.05 for three inhibitors and experimental %IE is in the range of 85 - 90 %, respectively. Mistry et al. [75] compared the ΔE values of two inhibitors and the inhibition efficiency and correlated with the experimental findings. In the present study, investigators obtained the ΔE value of 6.0833 eV and the experimental percentage efficiency is 95 %.

The dipole moment (μ) is an important parameter to find out the electronic distribution in a molecule and is used to rationalize the structure. Dipole moment can be defined as the product of magnitude of charges and the distance of separation between the charges. But many literatures explain the lack of agreement on the correlation between the dipole moment and inhibition efficiency [76, 77]. Despite lack of correlation, many literatures [78-80] reported that the molecule with lowest dipole moment has better inhibition efficiency. In the present study, investigators obtained the dipole moment of 7.1421 Debye.

The calculated fraction of electrons transferred from quinoline derivative molecule to iron is 0.2911. According to Lukovits [46], if $\Delta N < 3.6$, the inhibition efficiency increased with increasing electron-donating ability at the metal surface. In this study, the value of ΔN for Q2 was less than 3.6. This shows that the increase in inhibition efficiency was due solely to the electron-donating ability of Q2. The quinoline derivative was bound to the carbon steel surface, and thus formed inhibition adsorption layer against corrosion.

CONCLUSION

The main conclusions drawn from this study are 2-thioxo-1,2-dihydroquinoline-4-carboxylic (Q2) efficiently inhibits the corrosion of low carbon steel in 1 M HCl media. Te inhibition efficiency of Q2 increases with increasing the inhibitor concentration. Polarization curves reveal the Q2 is a mixed type inhibitor. Adsorption of the inhibitor

follows the Langmuir Isotherm. The EIS measurements suggest that Q2 molecules function by adsorption at metal surface thereby causing the decrease in C_{dl} values and increasing in R_{ct} values. Quantum chemical studies support the experimental results.

REFERENCES

- [1] M.M. Antonijevic, M.B. Petrovic, *Int. J. Electrochem. Sci.* **2008**, 3, 1.
- [2] Y.G. Avdeev, Y.I. Kuznetsov, *Russ. Chem. Rev.* **2012**, 81, 1133.
- [3] B.E.A. Rani, B.B.J. Basu, *Int. J. Corros.* **2012**, 2012, 1.
- [4] E.E. Oguzie, Y. Li, S.G. Wang, F. Wang, *RSC Adv.* **2011**, 1, 866.
- [5] N.S. Patel, S. Jauhari, G.N. Mehta, *Chem. Pap.* **2010**, 64, 51.
- [6] U.J. Naik, V.A. Panchal, A.S. Patel, N.K. Shah, *J. Mater. Environ. Sci.* **2012**, 3, 935.
- [7] A. Zarrouk, H. Zarrok, R. Salghi, B. Hammouti, F. Bentiss, R. Tourir, M. Bouachrine, *J. Mater. Environ. Sci.* **2013**, 4, 177.
- [8] A. Zarrouk, B. Hammouti, A. Dafali, F. Bentiss, *Ind. Eng. Chem. Res.* **2013**, 52, 2560.
- [9] H. Zarrok, A. Zarrouk, R. Salghi, Y. Ramli, B. Hammouti, M. Assouag, E. M. Essassi, H. Oudda and M. Taleb, *J. Chem. Pharm. Res.*, **2012**, 4, 5048.
- [10] A. Ghazoui, R. Saddik, N. Benchat, M. Guenbour, B. Hammouti, S.S. Al-Deyab, A. Zarrouk, *Int. J. Electrochem. Sci.*, **2012**, 7, 7080.
- [11] H. Zarrok, S. S. Al-Deyab, A. Zarrouk, R. Salghi, B. Hammouti, H. Oudda, M. Bouachrine, F. Bentiss, *Int. J. Electrochem. Sci.* **2012**, 7, 4047.
- [12] A. Zarrouk, B. Hammouti, H. Zarrok, M. Bouachrine, K.F. Khaled, S.S. Al-Deyab, *Int. J. Electrochem. Sci.*, **2012**, 6, 89.
- [13] H. Zarrok, K. Al Mamari, A. Zarrouk, R. Salghi, B. Hammouti, S. S. Al-Deyab, E. M. Essassi, F. Bentiss, H. Oudda, *Int. J. Electrochem. Sci.*, **2012**, 7, 10338.
- [14] H. Zarrok, H. Oudda, A. El Midaoui, A. Zarrouk, B. Hammouti, M. Ebn Touhami, A. Attayibat, S. Radi, R. Touzani, *Res. Chem. Intermed.* **2012**, 38, 2051.
- [15] A. Ghazoui, A. Zarrouk, N. Bencat, R. Salghi, M. Assouag, M. El Hezzat, A. Guenbour, B. Hammouti, *J. Chem. Pharm. Res.* **2014**, 6, 704.
- [16] H. Zarrok, A. Zarrouk, R. Salghi, H. Oudda, B. Hammouti, M. Assouag, M. Taleb, M. Ebn Touhami, M. Bouachrine, S. Boukhris, *J. Chem. Pharm. Res.* **2012**, 4, 5056.
- [17] A. Zarrouk, H. Zarrok, R. Salghi, R. Tourir, B. Hammouti, N. Benchat, L.L. Afrine, H. Hannache, M. El Hezzat, M. Bouachrine, *J. Chem. Pharm. Res.* **2013**, 5, 1482.
- [18] H. Zarrok, A. Zarrouk, R. Salghi, M. Assouag, B. Hammouti, H. Oudda, S. Boukhris, S.S. Al Deyab, I. Warad, *Der Pharm. Lett.* **2013**, 5, 43.
- [19] H. Zarrok, A. Zarrouk, R. Salghi, M. Ebn Touhami, H. Oudda, B. Hammouti, R. Tourir, F. Bentiss, S.S. Al-Deyab, *Int. J. Electrochem. Sci.* **2013**, 8, 6014.
- [20] D. Ben Hmamou, M.R. Aouad, R. Salghi, A. Zarrouk, M. Assouag, O. Benali, M. Messali, H. Zarrok, B. Hammouti, *J. Chem. Pharm. Res.* **2012**, 4, 3498.
- [21] M. Belayachi, H. Serrar, H. Zarrok, A. El Assyry, A. Zarrouk, H. Oudda, S. Boukhris, B. Hammouti, Eno E. Ebenso, A. Geunbour, *Int. J. Electrochem. Sci.* **2015**, 10, 3010.
- [22] H. Tayebi, H. Bourazmi, B. Himmi, A. El Assyry, Y. Ramli, A. Zarrouk, A. Geunbour, B. Hammouti, *Der Pharm. Chem.* **2014**, 6(5), 220.
- [23] H. Tayebi, H. Bourazmi, B. Himmi, A. El Assyry, Y. Ramli, A. Zarrouk, A. Geunbour, B. Hammouti, Eno E. Ebenso, *Der Pharm. Lett.* **2014**, 6(6), 20.
- [24] Y. ELoufir, H. Bourazmi, H. Serrar, H. Zarrok, A. Zarrouk, B. Hammouti, A. Guenbour, S. Boukhriss, H. Oudda, *Der Pharm. Lett.* **2014**, 6(4), 526.
- [25] H. Zarrok, A. Zarrouk, R. Salghi, H. Oudda, B. Hammouti, M. Ebn Touhami, M. Bouachrine, O.H. Pucci, *Port. Electrochim. Acta*, **2012**, 30, 405.
- [26] Y. ELouadi, F. Abridach, A. Bouyanzer, R. Touzani, O. Riant, B. ElMahi, A. El Assyry, S. Radi, A. Zarrouk, B. Hammouti, *Der Pharm. Chem.* **2015**, 7(8), 265.
- [27] F. Benhiba, H. Zarrok, A. Elmidaoui, M. El Hezzat, R. Tourir, A. Guenbour, A. Zarrouk, S. Boukhris, H. Oudda, *J. Mater. Environ. Sci.* **2015**, 6 (8), 2301.
- [28] M. Belayachi, H. Zarrok, M. Larouj, A. Zarrouk, H. Bourazmi, A. Guenbour, B. Hammouti, S. Boukhriss, H. Oudda, *Phys. Chem. News* **2014**, 74, 85.
- [29] L. Afrine, A. Zarrouk, H. Zarrok, R. Salghi, R. Tourir, B. Hammouti, H. Oudda, M. Assouag, H. Hannache, M. El Harti, M. Bouachrine, *J. Chem. Pharm. Res.* **2013**, 5, 1474.
- [30] A. Zarrouk, I. El Ouali, M. Bouachrine, B. Hammouti, Y. Ramli, E.M. Essassi, I. Warad, A. Aouniti, R. Salghi, *Res. Chem. Intermed.* **2013**, 39, 1125.

- [31] A. Zarrouk, B. Hammouti, H. Zarrok, R. Salghi, M. Bouachrine, F. Bentiss, S. S. Al-Deyab, *Res. Chem. Intermed.* **2012**, 38, 2327.
- [32] A. Zarrouk, B. Hammouti, H. Zarrok, S.S. Al-Deyab, I. Warad, *Res. Chem. Intermed.* **2012**, 38, 165.
- [33] M. El Hezzat, M. Assouag, H. Zarrok, Z. Benzekri, A. El Assyry, S. Boukhris, A. Souizi, M. Galai, R. Tourir, M. Ebn Touhami, H. Oudda, A. Zarrouk, *Der Pharm. Chem.* **2015**, 7(10), 77
- [34] S. EL Arouji, K. Alaoui Ismaili, A. Zerrouki, S. El Kadiri, Z. Rais, M. Filali Baba, M. Taleb, Khadijah M. Emran, A. Zarrouk, A. Aouniti, B. Hammouti, *Der Pharm. Chem.* **2015**, 7(10), 67.
- [35] M.J. Bahrami, S.M.A. Hosseini, P. Pilvar, *Corros. Sci.* **2010**, 52, 2793.
- [36] G. Moretti, G. Quartarone, A. Tassan, A. Zingale, *Electrochim. Acta* **1996**, 41, 1971.
- [37] R. Solmaz, G. Kardaş, M. Çulha, B. Yazıcı, M. Erbil, *Electrochim. Acta* **2008**, 53, 5941.
- [38] E. Lazarova, G. Petkova, R. Raicheff and G. Neykov, *J. Appl. Electrochem.* **2002**, 32, 1355.
- [39] M.A. Deyab, S.S. Abd El-Rehim, *Corros. Sci.* **2012**, 65, 309.
- [40] ASTM, G 31-72, American Society for Testing and Materials, Philadelphia, PA, **1990**.
- [41] Gaussian 03, Revision B.01, M. J. Frisch, et al., Gaussian, Inc., Pittsburgh, PA, **2003**.
- [42] W.J. Hehre, L. Radom, P.v.R. Schleyer, A.J. Pople, *Wiley-Interscience*, New York, **1986**.
- [43] J.F. Janak, *Phys. Rev. B* **1978**, 18, 7165.
- [44] R. Stowasser, R. Hoffmann, *J. Am. Chem. Soc.* **1999**, 121, 3414.
- [45] H. Ju, Z. Kai, Y. Li, *Corros. Sci.* **2008**, 50, 865.
- [46] I. Lukovits, E. Kalman, F. Zucchi, *Corrosion NACE* **2001**, 57, 3.
- [47] M. Sahin, S. Bilgic, H. Yilmaz, *Appl. Surf. Sci.* **2002**, 195, 1.
- [48] M.A. Migahed, A.A. Farag, S.M. Elsaed, R. Kamal, M. Mostfa, H. Abd El-Bary, *Mater. Chem. Phys.* **2011**, 125, 125.
- [49] M. Kaminski, Z. Szklarska-Smialowska, *Corros. Sci.* **1973**, 13, 557.
- [50] O. Olivares, N.V. Likhanova, B. Gomez, J. Navarrete, M.E. Llanos- Serrano, E. Arce, J.M. Hallen, *Appl. Surf. Sci.* **2006**, 252, 2894.
- [51] B. Hammouti, A. Zarrouk, S.S. Al-Deyab And I. Warad, *Orient. J. Chem.* **2011**, 27, 23.
- [52] M. Hosseini, S.F.L. Mertens, M.R. Arshadi, *Corros. Sci.* **2003**, 45, 1473.
- [53] E.S. Ferreira, C. Giacomelli, F.C. Giacomelli, A. Spinelli, *Mater. Chem. Phys.* **2004**, 83, 129.
- [54] A.O. Yuce, G. Kardas, *Corros. Sci.* **2012**, 58, 86.
- [55] M. Bouklah, N. Benchat, B. Hammouti, A. Aouniti, S. Kertit, *Mater. Lett.* **2005**, 60, 1901.
- [56] S. S. Abd El Rehim, H. H. Hassan, M. A. Amin, *Mater. Chem. Phys.* **2002**, 78, 337.
- [57] Q. Zhang, Y. Hua, *Mater. Chem. Phys.* **2010**, 119, 57.
- [58] K. F. Khaled, *Corros. Sci.* **2010**, 52, 2905.
- [59] H. Amar, T. Braisaz, D. Villemin, B. Moreau, *Mater. Chem. Phys.* **2008**, 110, 1.
- [60] A. H. Mehaute, G. Grep, *Solid State Ionics* **1989**, 910, 17.
- [61] R. Solmaz, E. Altunbas, G. Kardas, *Mater. Chem. Phys.* **2011**, 125, 796.
- [62] A. Chetouani, A. Aouniti, B. Hammouti, N. Benchat, T. Benhadda, S. Kertit, *Corros. Sci.* **2003**, 45, 1675.
- [63] M. Behpour, S. M. Ghoreishi, N. Soltani, M. Salavati-Niasari, *Corros. Sci.* **2009**, 51, 1073.
- [64] M. Hosseini, S. Mertens, M. Ghorbani, *Mater. Chem. Phys.* **2003**, 78, 800.
- [65] I. Naqvi, A.R. Saleemi, S. Naveed, *Int J Electrochem Sci.* **2011**, 6, 146.
- [66] D. Kumar Yadv, M.A. Quraishi, *Ind. Eng. Chem. Res.* **2012**, 51, 14966.
- [67] S. Ramachandran, B.L. Tsai, M. Blanco, H. Chen, Y. Tang, W.A. Goddard, *J. Phys. Chem. A* **1997**, 101, 83
- [68] I. Lukovits, K. Palfi, E. Kalman, *Corrosion* **1997**, 53, 915
- [69] E.H. El-Ashri, A. El-Nemr, S.A. Essawy, S. Ragub, *Electrochim. Acta* **2006**, 51, 3957
- [70] S.E. Nataraja, T.V. Venkatesha, K. Manjunatha, B. Poojary, M.K. Pavithra, H.C. Tandon, *Corros. Sci.* **2011**, 53, 2651.
- [71] G. Gao, C. Liang, *Electrochim. Acta* **2007**, 52, 4554.
- [72] B. Delley, *J. Chem. Phys.* **1990**, 92, 508.
- [73] A.S. Fouda, K. Shalabi, R. Maher, *Int. J. Advanced Res.* **2014**, 2, 1171.
- [74] M. Yadav, D. Behera, S. Kumar, R.R. Sinha, *Ind. Eng. Chem. Res.* **2013**, 52, 6318.
- [75] B.M. Mistry, N.S. Patel, S. Sahoo, S. Jauhari, *Bull. Mater. Sci.* **2012**, 35, 459.
- [76] M. Abdallah, S.T. Atwa, M.M. Salem, A.S. Fouda, *Int. J. Electrochem. Sci.* **2013**, 8, 10001.
- [77] L.M. Rodrigez-Valdez, A. Martinez-Villafane, D. Glossman-Mitnik, *J. Mol. Struct.* **2005**, 713, 65.
- [78] E.E. Ebenso, D.A. Isabirye, N.O. Eddy, *Int. J. Mol. Sci.* **2010**, 11, 2473.
- [79] K.F. Khaled, *Appl. Surf. Sci.* **2006**, 252, 4120.
- [80] N.A. Wazzan, F.M. Mahgoub, *Open J. Phys. Chem.* **2014**, 4, 6.